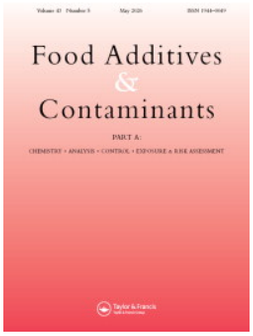

Food Additives & Contaminants: Part A

ISSN: 1944-0049 (Print) 1944-0057 (Online) Journal homepage: www.tandfonline.com/journals/tfac20

Migration of ionic and nanoparticulate zinc from nanocellulose/ZnO nanoparticle films: morphology-dependent behaviour and modelling

Ana Rita Mendes , Otmar Geiss , Ivana Bianchi , Jessica Ponti , Ana Matos , Cristina L. M. Silva & Fátima Poças

To cite this article: Ana Rita Mendes , Otmar Geiss , Ivana Bianchi , Jessica Ponti , Ana Matos , Cristina L. M. Silva & Fátima Poças (05 May 2026): Migration of ionic and nanoparticulate zinc from nanocellulose/ZnO nanoparticle films: morphology-dependent behaviour and modelling, Food Additives & Contaminants: Part A, DOI: 10.1080/19440049.2026.2633744

To link to this article: https://doi.org/10.1080/19440049.2026.2633744

Published online: 05 May 2026.

FOOD ADDITIVES & CONTAMINANTS: PART A
https://doi.org/10.1080/19440049.2026.2633744

Taylor & Francis
Taylor & Francis Group

Migration of ionic and nanoparticulate zinc from nanocellulose/ZnO nanoparticle films: morphology-dependent behaviour and modelling

Ana Rita Mendes[a], Otmar Geiss[b], Ivana Bianchi[b], Jessica Ponti[b], Ana Matos[c], Cristina L. M. Silva[a] and Fátima Poças[a,d]

[a]Universidade Católica Portuguesa, CBQF - Centro de Biotecnologia e Química Fina - Laboratório Associado, Escola Superior de Biotecnologia, Rua Diogo Botelho 1327, 4169-005 Porto, Portugal; [b]European Commission, Joint Research Centre (JRC), Ispra, Italy; [c]CISeD—Centro de Investigação em Serviços Digitais, Escola Superior de Tecnologia e Gestão de Viseu, Instituto Politécnico de Viseu, Viseu, Portugal; [d]CINATE, Escola Superior de Biotecnologia, Universidade Católica Portuguesa, Porto, Portugal

ABSTRACT

The incorporation of zinc oxide nanoparticles (ZnO NPs) into biopolymers has gained attention for active food packaging due to their antimicrobial properties. However, potential Zn migration associated with safety concerns remains underexplored, particularly in non-regulated bio-based polymers. In this study, Zn migration from nanocellulose (NC) films incorporating spherical-, flower- and sheet-shaped ZnO NPs was evaluated, in ionic and nanoparticulate forms. Migration tests were conducted using water and ethanol 10% as food simulants under different time-temperature conditions. Zinc release was quantified using complementary analytical and microscopic approaches, and Fick's second law and Weibull models were employed to describe the migration kinetics. Migration behaviour was influenced by nanoparticle morphology, simulant type, and temperature. Zinc migrated predominantly as Zn^{2+}, with minimal nanoparticle contribution, although distinction from cellulose fibres proved challenging. NC films containing flower-shaped nanoparticles exhibited the highest Zn migration, yet migration levels for all films remained below the European specific migration limit. Water promoted higher migration than ethanol, and unexpectedly, Zn migration was lower at 60 °C compared to 23 °C, likely due to matrix effect. Fickian fits yielded diffusion coefficients in the range 10^{-16}–10^{-15} m^2 s^{-1}, while Weibull $\beta < 1$, confirmed diffusion-controlled release. These findings confirm the potential of NC/ZnO nanocomposites for food packaging applications and highlight the importance of combining multi analytics with kinetic modelling to support safety assessment.

Abbreviations: AAS: atomic absorption spectroscopy; AF4: asymmetric flow field-flow fractionation; Ag NPs: silver nanoparticles; D: diffusion coefficient; DLS: dynamic light scattering; EDS: energy dispersive X-ray spectroscopy; EFSA: European food safety authority; FCMs: food contact materials; FFF: field flow fractionation; ICP-MS: inductively coupled plasma mass spectrometry; K: partition coefficient; LDPE: low density polyethylene; MALS: multi-angle light scattering; MSE: mean squared error; NC: nanocellulose; NPs: nanoparticles; PBAT: poly(butylene adipate-co-terephthalate); PLA: polylactic acid; PS: polystyrene; ROS: reactive oxygen species; SEM: scanning electron microscopy; SML: specific migration limit; spICP-MS: single particle inductively coupled plasma mass spectrometry; TEM: transmission electron microscopy; TPS: thermoplastic starch; ZnO NPs: zinc oxide nanoparticles; ZnO-FL: flower-like zinc oxide nanoparticles; ZnO-SH: sheet-like zinc oxide nanoparticles; ZnO-SP: spherical zinc oxide nanoparticles

ARTICLE HISTORY
Received 14 January 2026
Accepted 11 February 2026

KEYWORDS
Zinc oxide nanostructures, ionic/nanoparticulate migration; nanocellulose films; migration modelling; food contact materials

Introduction

Food packaging plays a crucial role not only in preserving food quality and safety but also in ensuring security during storage and distribution. Increasing environmental concerns associated with conventional plastics have driven the search for eco-friendly alternatives, particularly bio-based systems. In parallel, growing attention has been given to the potential migration of substances from packaging into food, which can compromise both safety and regulatory compliance (Tabassum et al. 2023; Wang et al. 2025; Zhang et al. 2025). Among natural polymers, cellulose stands out due to its abundance, renewability, and excellent

CONTACT Fátima Poças fpocas@ucp.pt Universidade Católica Portuguesa, CBQF - Centro de Biotecnologia e Química Fina - Laboratório Associado, Escola Superior de Biotecnologia, Rua Diogo Botelho 1327, 4169-005 Porto, Portugal.

film-forming capabilities (Santos et al. 2021). Cellulose derived from plant sources are extensively employed in packaging materials, including paper, paperboard, moulded pulp articles, and regenerated cellulose transparent films (Garrido-Romero et al. 2022). Nanocellulose (NC) presents long, flexible, and entangled fibres with high surface area, mechanical strength, and good compatibility with other components and has emerged as an attractive matrix for packaging materials (Silva et al. 2020). Several studies have demonstrated the successful incorporation of cellulose into bio-based coatings for food contact materials (FCMs) (Sun et al. 2024; Singh et al. 2025; Zhang et al. 2025).

Recent advances in food packaging have explored the use of functional additives, such as organic compounds, natural extracts, and inorganic nanoparticles (NPs), leading to active materials with enhanced preservation capacity. The incorporation of nanoscale fillers into polymeric matrices has gained particular attention due to the unique properties of nanomaterial (Anvar et al. 2021; Herrera-Rivera et al. 2024; Parab et al. 2025). Among these materials, zinc oxide nanoparticles (ZnO NPs) have attracted significant attention due to their antimicrobial properties, UV protection, chemical stability, and compatibility with bio-based polymers (Lebaka et al. 2025). ZnO NPs can be synthesised in distinct morphologies and sizes, including spherical, flower, and sheet structures, each exhibiting distinct physicochemical and functional properties that may affect their release migration behaviour (Kwabena et al. 2021). Their antimicrobial efficacy arises mainly from zinc ion release and reactive oxygen species (ROS) generation, resulting in microorganism membrane damage and cell death (Kumar et al. 2017; Mendes et al. 2025). When incorporated into biopolymer matrices, ZnO NPs can improve mechanical, barrier, and antimicrobial performance, thereby extending food shelf life (Gao et al. 2025; Karuppan Perumal et al. 2025). NC-based materials complemented with ZnO NPs have been reported to exhibit outstanding mechanical strength, UV protection, and antibacterial activity (Farooq et al. 2020; Soares Silva et al. 2023a).

Despite these functionalities, the migration of nanoparticles from packaging materials into food raises concerns regarding safety and regulation compliance. While the antimicrobial properties of ZnO NPs are well documented (Anvar et al. 2021; Kim et al. 2022), fewer studies have addressed their potential migration, particularly in non-plastic materials. Uncontrolled zinc release may exceed regulatory thresholds or pose toxicological risks, and nanoparticles may also induce unwanted chemical reactions due to their high surface-to-volume ratio and surface chemistry (Habib et al. 2024). Although ZnO NPs have received a positive safety evaluation to be used in plastics packaging applications as ultraviolet light absorbers (EFSA 2016), uncertainties remain regarding the potential biological interactions and toxic effects when applied to bio-based polymers. As for other mass transfer processes, ZnO NPs migration is influenced by several factors, including properties of the migrant, material characteristics, the nature of the food matrix, and the contact conditions. In general, migration refers to the transfer of substances from the packaging to food by physical processes. The most typical mechanism is Fickian diffusion, governed by concentration gradients across the material matrix, which has been extensively applied to migration of monomers and conventional additives from plastics (Störmer et al. 2017; Poças 2018; Seref and Cufaoglu 2025). However, other processes may be particularly relevant for nanomaterials, such as matrix degradation, adsorption/desorption, dissolution, and mechanical abrasion (Noonan et al. 2014). To describe these transfer processes, mathematical models have been proposed, including mechanistic models, based on Fick's laws (Brandsch et al. 2002; Poças et al. 2008) and empirical models, such as the Weibull equation (Poças et al. 2012). Other approaches have been reported, including first-order kinetics, Korsmeyer–Peppas, Elovich-type models, and Arrhenius-type relationships to describe the effect of temperature in the model parameters (Kim et al. 2019). However, most studies have focused on conventional plastics, while applications to non-plastic bio-based systems remain scarce. Only a few studies have investigated the migration of components in

cellulose/paper materials (Zülch and Piringer 2010; Poças et al. 2011; Hauder et al. 2013; Cai et al. 2017), and none have addressed the migration of ZnO NPs, underscoring the relevance of the present study.

For inorganic nanoparticles, migration and release mechanisms are poorly understood. In such cases, the migrant particle may change in size and/or may dissolve upon being transferred into the food medium. One major challenge involving metallic nanoparticles, such as zinc oxide, is the difficulty in distinguishing between ionic zinc (Zn^{2+}) and nanoparticulate ZnO, since quantification in complex matrices is hindered by matrix effects and requires highly sensitive analytical techniques. Currently, no standardised protocol exists for NPs migration testing. Analytical tools include Inductively Coupled Plasma Mass Spectrometry (ICP-MS), Single Particle ICP-MS (spICP-MS) and Atomic Absorption Spectroscopy (AAS), complemented by methods such as Dynamic Light Scattering (DLS), Field Flow Fractionation (FFF), Transmission Electron Microscopy (TEM) and Scanning Electron Microscopy (SEM) with Energy Dispersive X-ray Spectroscopy (EDS) (Schmidt et al. 2011; Corps Ricardo et al. 2021). Despite the availability of these techniques, reported migration studies remain limited regarding the form in which the nanoparticles migrate and sometimes present contradictory results (Souza and Fernando 2016; Störmer et al. 2017).

From a regulatory perspective, the European Commission established a specific migration limit (SML) for zinc in plastic FCMs of 5 mg kg^{-1} of food, applying only to ionic zinc (European Commission 2016). This regulation and the guidelines of European Food Safety Authority (EFSA) indicate that the risk assessment of nanoparticles must be conducted on a case-by-case basis and therefore no SML is established (More et al. 2021a, 2021b). EFSA concluded that uncoated ZnO NPs dissolve under gastric conditions, releasing Zn^{2+}. Thus, toxicological assessment could rely on soluble zinc, although uncertainties remain regarding the state of intact particles (EFSA 2015). While no nanoparticulate migration has been reported in plastics materials (EFSA 2016), behaviour may differ substantially in porous matrices such as cellulose (Poças and Franz 2018).

Given these challenges, it is critical to clarify ZnO migration mechanisms in NC films, which are increasingly proposed as sustainable alternatives to plastics. A limited number of studies has investigated this issue (Sharaby et al. 2022; Soares Silva et al. 2023b), and further investigation is required to determine whether, and to what extent, nanoparticles can migrate and to assess the potential impacts on human health. This study investigates Zn migration from NC films reinforced with ZnO NPs of three morphologies (spherical, flower, and sheet). A multi-technique analytical approach was applied to distinguish between ZnO NPs and Zn^{2+} migration, and to study the influence of particle morphology, food simulant type, and temperature on zinc migration behaviour. Mechanistic (Fick) and empirical (Weibull) models were applied to describe migration kinetics. By integrating advanced analytical tools with mathematical modelling, this work aims to improve understanding of NPs migration and support the development of safe and functional bio-based active packaging systems.

Materials and methods

Preparation of fibrillated nanocellulose/zinc oxide nanoparticle films

The ZnO NPs used in this study were previously synthesised in-house with three morphologies—spherical (ZnO-SP), flower (ZnO-FL), and sheet shape (ZnO-SH), and have already been fully characterised in terms of their physicochemical and functional properties (Mendes et al. 2024, 2025).

The solvent casting method was employed to prepare NC/ZnO films. The fibrillated NC used for the films was Valida S231C 3% (Sappi Biochemtech BV, Maastricht, Netherlands), a biodegradable material derived from wood pulp, sourced from sustainably managed forests, with particle sizes in the nano- and micrometer range. According to the supplier's technical datasheet, the fibrils width ranged from 20 to 60 nm, with a length distribution of <5 µm (10%), <12 µm (50%) and <31 µm (90%). NC suspension of 1% (w/v) was prepared in ultrapure water (Milli-Q) and mixed for 30 min at room temperature. Glycerol

(Sigma-Aldrich, St. Louis, MO, US), used as a plasticiser, was added at 5% (w/w based in dry NC) under continuous stirring. Subsequently, 10% (w/w based in dry NC) of each ZnO NPs type was incorporated into the NC solution and stirred for an additional 30 min. Approximately 32 mL of the resulting mixture was poured into a 10 × 10 cm support and left to dry at 23 °C and 50% relative humidity for 48 h. Once dried, the film samples were designated as NC/ZnO-SP, NC/ZnO-FL, and NC/ZnO-SH, corresponding to each ZnO NPs variant (spherical, flower and sheet shape, respectively). NC films without the addition of ZnO NPs were prepared as a control following the same protocol.

Migration testing

Zinc migration can occur either through dissolution as ionic zinc (Zn^{2+}) or as ZnO NPs directly into the food simulant. Therefore, one of the objectives of this study was to differentiate between these two types of transfer. Analysing migratory compounds in real food products can be complex, costly, and time-consuming due to the heterogeneous nature of food matrices. Therefore, food simulants were used as substitutes in migration studies. After the migration step, the simulant was treated to estimate the mass concentration of zinc migrating in the two forms. The simulant was analysed before filtration/deposition (total zinc) and after filtration/deposition (ionic zinc). Both fractions were acidified prior to analysis. Two analytical techniques were used to measure the zinc—AAS and ICP-MS. Additionally, spICP-MS was also conducted to determine the number of particles migrating.

The migration tests were performed in conditions adapted from the EU Regulation 10/2011, with food simulants (distilled water and/or ethanol 10% (v/v) in distilled water). Food simulant A (ethanol 10%) is the official simulant for aqueous foods and should therefore be used for migration testing. Water was also a simulant foreseen in previous versions of the Regulation. For food matrices with high water activity, this simulant is widely used in research as a simplified aqueous medium. For acidic foods (pH < 4.5), food simulant B (acetic acid 3%) is required. Vegetable oil should be used to simulate contact with fatty food. However, given the effect of low pH in rapid migration of metal migrants in acidic conditions and the very low migration to oil, these two simulants corresponding to extreme migration cases were not used. The films were immersed in the food simulant using a solid-to-liquid ratio of 2.5 dm^2 L^{-1}. The contact period was 10 days or up to 35 days, with multiple sampling time points throughout the contact period to monitor the kinetic release profiles, depending on the temperature of test (8 °C, 23 °C, and 60 °C). The experiments were run with three independent replicates of each film and for each sampling point. A control sample (neat NC) was included in the experiments, and all zinc measurements in these samples were below the limit of detection (LOD). Table 1 summarises the experimental conditions and analytical techniques used to evaluate ZnO NPs migration across study objectives.

Differentiating ionic Zn^{2+} and ZnO NPs in food simulants

A schematic representation of the experimental procedure is provided in Figure 1.

Table 1. Experimental conditions and analytical techniques for ZnO NPs migration studies.

Objective of test	ZnO NPs	Food simulant	Conditions T/t (°C/days)	Analytical technique
Differentiating ionic Zn^{2+} and ZnO NPs	ZnO-SP ZnO-FL ZnO-SH	Water 10% EtOH	60 °C and 20 d (multiple time points) 60 °C and 10 d	AAS ICP-MS spICP-MS TEM
Effect of food simulant on total Zn migration	ZnO-SP ZnO-FL ZnO-SH	Water 10% EtOH	60 °C and 20 d (multiple time points)	AAS
Effect of temperature on total Zn migration	ZnO-SP	Water	8, 23, 60 °C 35 d (multiple time points)	AAS

Abbreviations: AAS: atomic absorption spectroscopy; ICP-MS: inductively coupled plasma mass spectrometry; spICP-MS: single particle inductively coupled plasma mass spectrometry; TEM: transmission electron microscopy

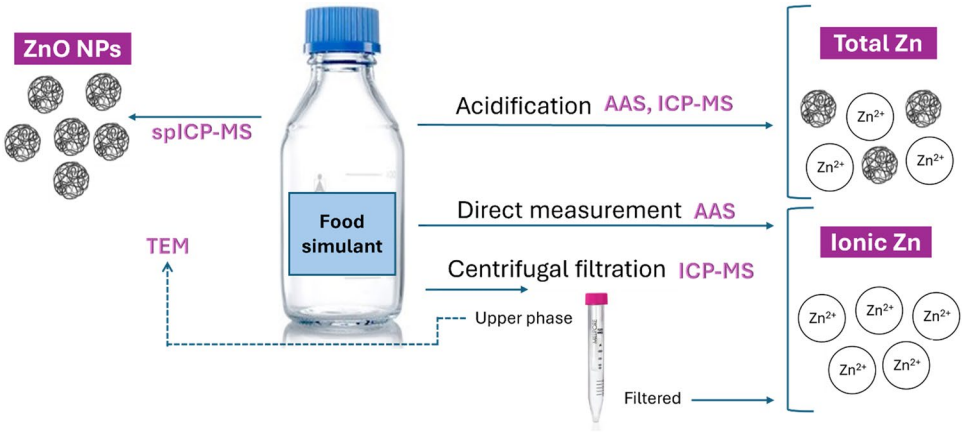

Figure 1. Experimental scheme of food simulant measurements for determining total Zn, ionic Zn, and ZnO NPs, using AAS, ICP-MS, spICP-MS and TEM as analytical techniques.

Ionic zinc

The simulants were first analysed to quantify Zn^{2+} using the following approaches: (i) the particles were allowed to settle for 15 min and the upper part of the migration solution was analysed by AAS (direct measurement in Figure 1), and (ii) 5 mL of the migration solution were passed through a 10 kDa Amicon centrifugal filter (Merck Millipore Ltd, Ireland, Amicon Ultra-4, 10 K, 1.42 nm equivalent size), which retains the nanoparticles in the upper part (centrifugation at 4800 rpm for 10 min, at room temperature). The ionic Zn in the filtrate (bottom part) was then quantified by ICP-MS.

Total zinc (ionic and nanoparticles)

The simulants were acidified to determine the total zinc content, by adding 1% (v/v) of 65% nitric acid (HNO_3) (Panreac, Barcelona, Spain). The solutions were centrifuged for 10 min at 4800 rpm, at room temperature (Hermle Italia GmbH, Rodano, Italy, Model Z 206 A) to remove cellulose fragments and avoid clogging the nebuliser of the equipment, before analysis with ICP-MS.

Quantification of zinc by atomic absorption spectroscopy and inductively coupled plasma mass spectrometry

Atomic absorption spectroscopy

The concentration of Zn in food simulants was quantified by AAS according to standard EN 14084, using an atomic absorption spectrophotometer (Perkin Elmer Aanalyst 400, Waltham, MA), equipped with a zinc cathode lamp ($\lambda = 213.9$ nm). Zinc working solutions (0–0.50 mg L^{-1}) were previously prepared for each food simulant by diluting a 1000 mg L^{-1} stock solution with a 1% (v/v) HNO_3 solution. When necessary, the samples were diluted with ultrapure water to achieve an absorbance signal within the Zn concentration range of 0–0.50 mg L^{-1}. Five readings were made for all samples and working solutions. The system suitability was evaluated by determining the limit of detection (LOD: 0.008 mg L^{-1}), the limit of quantification (LOQ: 0.025 mg L^{-1}), and recovery (90%–110%).

Inductively coupled plasma mass spectrometry

Standards and sample-solutions were analysed with a Perkin Elmer Nexion 300D ICP-MS (isotopes: Zn-66, Sc-45, dwell time: 50 ms, sweeps per reading: 20) equipped with a Meinhard concentric nebuliser, a baffled glass cyclonic spray chamber and a standard quartz torch (2.0 mm injector i.d.). Calibration curves of ionic Zn standard solutions were prepared in 1% nitric acid for the migration tests with simulant water and in 1% ethanol/1% nitric acid for the migration tests with simulant 10% ethanol, in a concentration range of 0–0.1 mg L^{-1}. All solutions were prepared gravimetrically, using an intermediate ionic zinc-solution of 10 mg L^{-1}. The intermediate solution was obtained by diluting a commercially available 1000 mg L^{-1} Zn standard solution (Sigma-Aldrich, St. Louis, MO, US). The ionic Zn standard solutions for water simulant contained 0.05 mg L^{-1} of scandium as internal

standard. The system had an LOD and LOQ of 1×10^{-6} mg L^{-1} and 3×10^{-6} mg L^{-1}, respectively, and the recovery of ionic zinc was higher than 95%.

Number of particles determined by single particle inductively coupled plasma mass spectrometry

The presence of ZnO NPs were determined by measuring the undiluted migration solution (Figure 1) in single particle ICP-MS mode. For the setting of all parameters and data acquisition, the Nano Application Module of Syngistix™ software version 2.5 was used. The dwell time was set at 100 µs and the total data acquisition time at 60 s (scan-time). The exact flow rate of the peristaltic pump required for the determination of the transport efficiency was measured gravimetrically and was 0.154 mL min^{-1} when aspirating ultrapure water as migration medium and 0.145 mL min^{-1} when aspirating 10% ethanol as migration medium. The transport efficiency was determined following the particle size method (Pace et al. 2011; Geiss et al. 2022) using the combination of ionic gold and gold NPs. For the determination of ZnO NPs, the zinc-66 isotope was monitored setting the mass fraction to 81.1%, the density to 7.14 g cm^{-3} and the ionisation efficiency to 100%. A 5-point calibration curve ranging from 0 to 50 µg L^{-1} zinc dissolved in ultrapure water and in 10% ethanol was used for the size calibration.

Transmission electron microscopy

The presence of migrated ZnO NPs in distilled water food simulant after 10 days of contact at 60 °C was evaluated by TEM (JEOL-JEM 2100, JEOL, Italy). As described above, the entire volume of the migration solution was filtered using 10 kDa Amicon centrifugal filters, and the particles were retained in the upper section of the filters. After complete filtration, 3 µL of the retained fraction (around 10 µL) were manually deposited on Formvar carbon-coated 200 mesh copper grids (Agar Scientific, London, UK), pre-treated by glow discharge (EM ACE600; 10 mV, 30 s, Leica, Italy), left to dry overnight in a desiccator, and images acquired by TEM at 120 kV.

In addition, each NC/ZnO film was analysed by directly depositing a piece of each film before and after incubation into distilled water food simulant at 60 °C during 10 days of contact. Specifically, a 3 µL drop of distilled water was dropped on glow discharged pre-treated grids and a piece of film gently deposited on it. The samples were left to dry overnight in a desiccator and analysed them by TEM at 120 kV.

Migration mathematical modelling

The migration kinetics of Zn from NC/ZnO films into water simulant at 60 °C were evaluated by fitting the experimental data to Fick's second law of diffusion (mechanistic) and to the Weibull model (empirical).

The diffusion of a substance in a polymeric medium can be described by Fick's second law (Eq. (1)):

$$\frac{\partial C_A^P}{\partial t} = D_A^P \frac{\partial^2 C_A^P}{\partial x^2} \quad (1)$$

where C_A^P represents the concentration of the migrant A in the packaging material P, t is the time, x is the linear direction of the mass transport, and D_A^P is the diffusion coefficient of migrant A in the packaging material (Crank 1986).

Considering a planar sheet of thickness δ, with an initial uniform concentration of the migrant in the material and initial concentration of migrant in the food of zero, the analytical solution is expressed by the infinite series (Eq. (2)). Under these boundary conditions, migration is controlled exclusively by diffusion within the polymer, while the well-mixed food (or simulant) phase acts as a perfect sink, with no resistance at the interface.

$$\frac{M_t}{M_\infty} = 1 - \sum_{n=0}^{\infty} \frac{8}{(2n+1)^2 \pi^2} \exp\left[-\frac{(2n+1)^2 \pi^2}{\delta^2} Dt \right] \quad (2)$$

where M_t is the total Zn migration (mg kg^{-1}) at time t (s), M_∞ is the Zn migration at equilibrium (mg kg^{-1}), δ is the film thickness (m), and D is the diffusion coefficient of Zn in the composite film (m^2 s^{-1}).

In the field of plastic FCM, the diffusion (D) and partition (K) coefficients are generally

estimated using empirical correlations and assumed upper-bound values. These parameters describe the mass transfer process according to Fick's law, where D represents the rate at which the migrant diffuses through the polymeric matrix, and K defines the distribution of the migrant between the polymer and food (or simulant) phase at equilibrium. The diffusion coefficient is typically calculated based on the migrant molecular weight and temperature. The partition coefficient, when no experimental values are available, is simply taken as 1 if the migrant is very soluble in the food phase or as 1 000 for systems with low solubility (Poças et al. 2008; Hoekstra et al. 2015). The worst-case approach ensures that the modelled migration does not underestimate reality and thus provides a conservative basis for compliance assessment (Piringer and Baner 2008).

The experimental migration data were also fitted to the Weibull model (Eq. (3)), which has been widely used to describe the release of compounds in various biological systems (Bayer 2023). It expresses the fraction of Zn released as:

$$\frac{M_t}{M_\infty} = 1 - \exp\left[-\left(\frac{t}{\tau}\right)^{\beta}\right] \quad (3)$$

where M_t and M_∞ represents the total Zn migrated (mg kg^{-1}) at time t (s) and at equilibrium, respectively; τ is the scale parameter (time constant), and β defines the shape of the curve ($\beta = 1$ corresponds to an exponential function; $\beta > 1$ indicates a sigmoid release profile with an inflection point; and $\beta < 1$ describes a curve with a rapid initial stage (burst release) followed by a slower release.

Data handling and statistical analysis

Statistical analysis was performed using IBM SPSS Statistics (version 28), GraphPad Prism (version 8.4.2) and Microsoft Excel. Data were expressed as the mean values ± standard deviation.

Two-way paired sample analysis of variance was applied to assess the effect of ZnO NPs morphology on Zn migration over time, comparing water vs. water/HNO_3, as well as ethanol 10% vs. ethanol 10%/HNO_3. Regression models were applied to estimate the evolution of Zn migration over time. A two-sided $p < 0.05$ was considered statistically significant. Paired samples t-test was applied to compare the Zn migration of the unfiltered and filtered fractions of each food simulant in the ICP-MS experiment.

Non-linear regression for both Fick and Weibull models was performed by minimising the mean squared error (MSE) between experimental and predicted values using an iterative optimisation algorithm. The goodness of fit was evaluated through the coefficient of determination (R^2) and MSE.

Results and discussion

Zn migration: ionic vs nanoparticulate mass fractions

Results are presented in Figure 2, showing the Zn mass concentration in both food simulants before and after acidification, for the NC films with different ZnO NPs morphologies. Acidification led to results with slightly higher Zn concentration, and the minimal differences between acidified and non-acidified samples suggest that a small fraction of zinc migrated in nanoparticulate form, with the majority occurring as ionic Zn. The Zn migration pattern was similar for both food simulants, and the migration profile was influenced by the morphology of ZnO NPs. For the film with spherical particles (NC/ZnO-SP), Zn migration showed a gradual increase over time, stabilising after approximately 1 day for ethanol 10% (in the first 24 h, the Zn migration rate was estimated at 0.83 mg Zn kg^{-1} simulant, 95%CI ranging from 0.483 to 1.165, $p < 0.001$) and 7 days for water food simulant (average daily increase estimated at 0.198 mg Zn kg^{-1}, 95%CI ranging from 0.164 to 0.234, $p < 0.001$). For the film with flower morphology (NC/ZnO-FL), an initial pronounced increase in Zn migration was observed for both food simulants, followed by a statistically significant decrease ($p < 0.001$) and stabilisation until 20 days. The NC/ZnO-FL migration profile exhibited irregular fluctuations in Zn release into the water simulant over time, which may be attributed to Zn reabsorption, precipitation, or interactions with the food simulant. This apparently

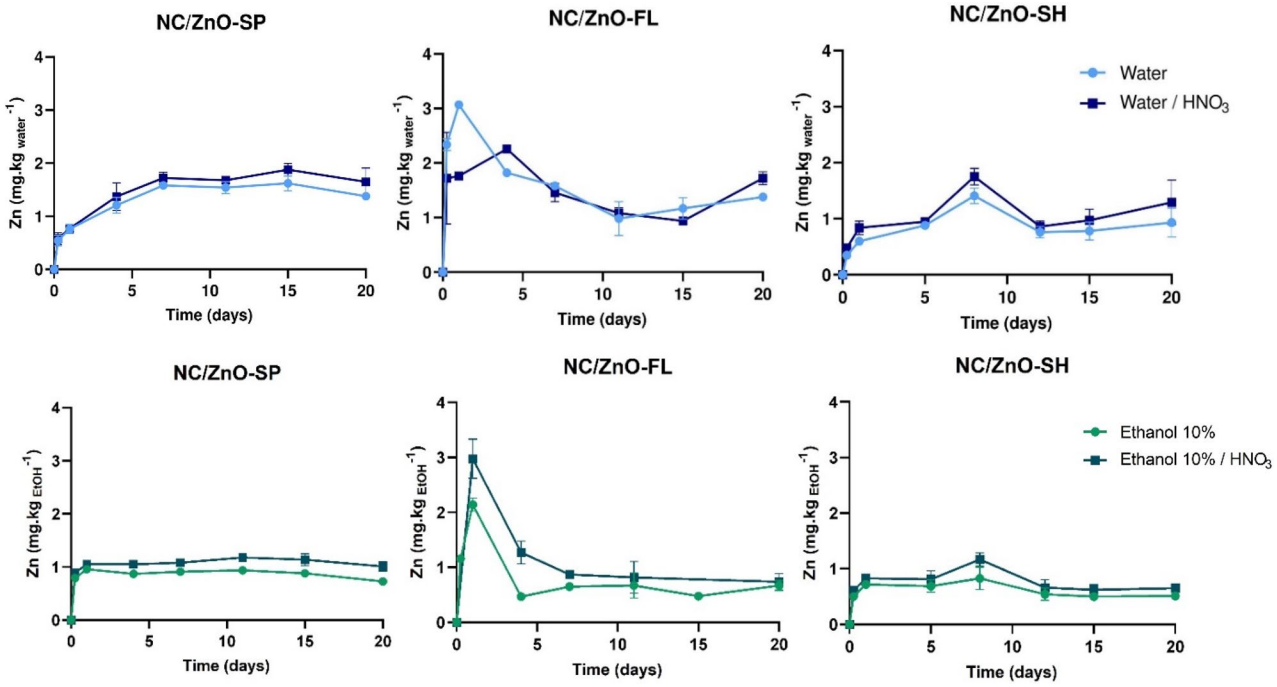

Figure 2. Total and ionic Zn migration from NC/ZnO-SP, NC/ZnO-FL, and NC/ZnO-SH composites into water and ethanol 10% food simulant at 60 °C over 20 days, before and after acidification, using AAS. NC/ZnO-SP—nanocellulose film with spherical ZnO NPs; NC/ZnO-FL—film with flower-like ZnO NPs; NC/ZnO-SH - film with sheet-like ZnO NPs.

reabsorption behaviour was already reported in the literature (Soares Silva et al. 2023a; Singh et al. 2024). The film with sheet particles (NC/ZnO-SH) exhibited small variations over time, reaching a maximum migration value on the 8th day, remaining constant thereafter. It has been reported that the dissolution kinetics of ZnO is influenced by physicochemical characteristics such as particle morphology, size, aggregation, and specific surface area (Cardoso et al. 2021), which can explain the different migration profiles here reported.

The NC/ZnO-FL film exhibited the highest Zn release into the water simulant (3.07 mg kg^{-1}) compared to the films with different ZnO NPs shapes. The migration levels for all nanocomposites remained below the SML of 5 mg kg^{-1} of food for soluble ionic zinc, as established by European Plastics Regulation (EU) 2016/1416, which amends and corrects Regulation (EU) No. 10/2011 (European Commission 2016). It suggests that ionic Zn migration from the films remains within acceptable safety limits, alleviating health concerns regarding potential exposure, despite being legislation applicable to plastic packaging. However, migration in nanoparticulate form still requires verification, and therefore complementary techniques were used (Sections Determination of particle number concentration by spICP-MS and Microscopic visualisation of particles in films and food simulants via Transmission Electron Microscopy). The controlled Zn release could be beneficial for antimicrobial applications in food packaging, as previously reported for these nanoparticles (Mendes et al. 2025) where achieving a balance between functionality and regulatory compliance is essential.

According to Figure 2, some reabsorption of the migrated Zn was observed for NC/ZnO-FL, which could be attributed to interactions between the released Zn species and the cellulose matrix, a phenomenon previously reported in cellulose-based materials (Poças et al. 2011; Soares Silva et al. 2023b). Such phenomena can be attributed to changes in the cellulose matrix (swelling, restructuring, alteration of interfacial area) that influence the adsorption, reabsorption, and migration dynamics of nanoparticles (Österberg et al. 2023). Furthermore, a study demonstrated that cellulose films could adsorb metal ions through multiple mechanisms, including electrostatic attraction and chaotropic effects, highlighting the complexity of metal ion interactions with bio-based materials (Paul et al. 2024).

The acidification method provides only a qualitative assessment of the presence of Zn in nanoparticulate form. In fact, the difference between the values before and after acidification may be influenced by other factors, such as reabsorption, precipitation, or interactions with the food simulant. Therefore, although these results indicate ZnO NPs migration, the exact quantity cannot be determined using this approach.

The results obtained by ICP-MS for the total and ionic Zn migration after 10 days of contact with water and ethanol 10% food simulants are presented in Figure 3, using paired dot plots and boxplots of $\Delta Zn = Zn_{total} - Zn^{2+}$. For all samples, positive values of ΔZn were observed, meaning that quantified migration in the unfiltered simulant (total zinc) is slightly higher than filtered fraction (ionic). These minimal differences suggest that migration occurred predominantly in ionic form, with small contribution from ZnO NPs, corroborating the results previously obtained by AAS. In the water simulant, there is statistical evidence that total Zn is significantly higher than ionic Zn for all ZnO NPs shapes ($p < 0.05$ for ZnO-SP and ZnO-FL; $p < 0.01$ for ZnO-SH). ZnO-FL exhibited the highest Zn migration (approximately 0.6 mg L^{-1} for total Zn and 0.5 mg L^{-1} for ionic Zn), consistent with the largest difference observed in boxplots (~0.1 mg L^{-1}), while ZnO-SP and ZnO-SH showed smaller differences (<0.06 mg L^{-1}). In the ethanol 10% simulant, a statistical difference is detected only for ZnO-FL ($p < 0.05$), whereas ZnO-SP and ZnO-SH showed no significant differences, confirming that migration in this simulant occurred predominantly in ionic form. Overall, the differences between total and ionic Zn in ethanol food simulant were smaller and more similar across morphologies, compared to water. Notably, all Zn levels for both food simulants remained below the SML, complying with current legislation.

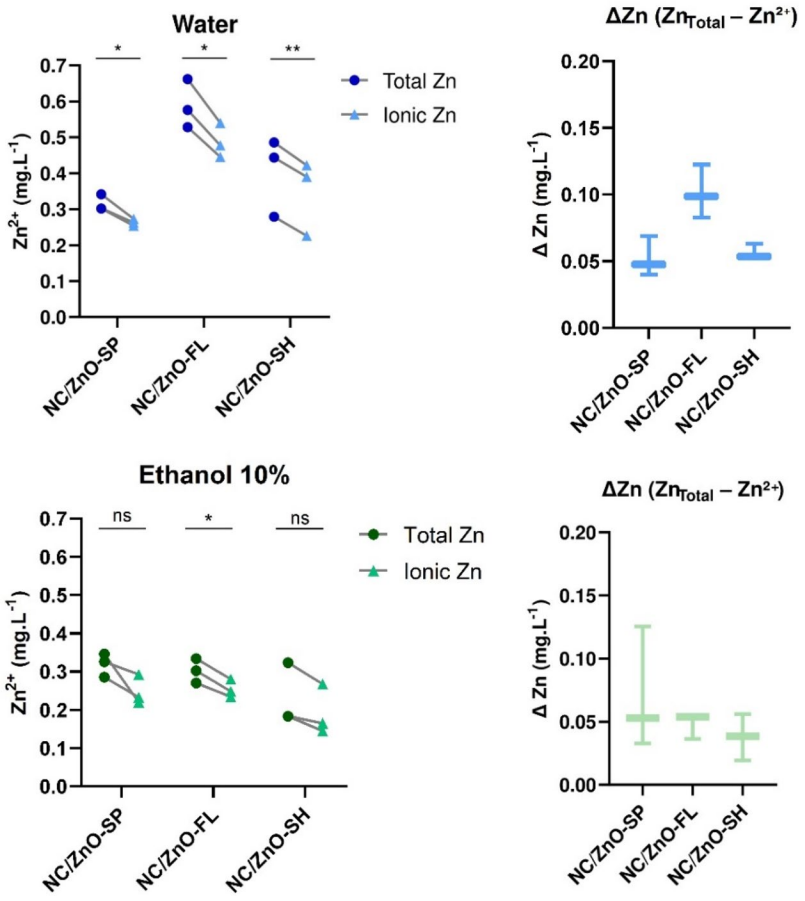

Figure 3. Comparison of total Zn and ionic Zn migration from NC/ZnO NPs films into water and ethanol 10% food simulants, using ICP-MS. Left: paired plots showing individual values (lines connect paired total and ionic Zn, $n = 3$); Right: boxplots of the ΔZn ($Zn_{Total} - Zn^{2+}$). Statistical differences were evaluated by paired sample t-test (*$p < 0.05$, **$p < 0.01$, ns = not significant). NC/ZnO-SP - nanocellulose film with spherical ZnO NPs; NC/ZnO-FL - film with flower-like ZnO NPs; NC/ZnO-SH - film with sheet-like ZnO NPs.

The results obtained by AAS were approximately 30% higher than those obtained by ICP-MS (Figure S1). This difference can be attributed to the distinct separation principles of each method. In AAS, the analysis was performed directly after nanoparticle deposition, without any filtration step, meaning that both dissolved ions and undeposited ZnO NPs present in the supernatant could contribute to the measured value. In contrast, ICP-MS was applied after centrifugal filtration using a 10 kDa membrane, which retains nanoparticles in the upper fraction, allowing only ionic Zn^{2+} to pass through. Therefore, the more efficient separation is the ICP-MS approach likely led to lower measured concentrations.

Differentiating between ionic and nanoparticulate forms remains a challenge today. Most studies use conventional AAS or ICP-MS for Zn quantification in food simulants without distinguishing between ZnO NPs and Zn^{2+} (Panea et al. 2014; Huang et al. 2017). Choleva et al. (2019) developed an alternative approach for silver nanoparticles (Ag NPs), involving a selective extraction step to separate both fractions. Ag NPs were partitioned into dispersed octanol droplets from the aqueous phase, and these droplets were then re-dispersed into a strongly acidic and oxidising aqueous medium to dissolve the Ag NPs into Ag^{+} ions, enabling quantification by AAS. Another study developed a quantitative analytical method for detecting ZnO NPs in environmental waters using cloud point extraction combined with ICP-MS. The use of a masking agent minimised Zn^{2+} interference, ensuring the selective extraction of ZnO NPs in their nanoform (Yang et al. 2021). Despite methodological differences, these approaches highlight the current challenge in clearly distinguishing between ionic and nanoparticulate migration. Further research is still needed to establish standardised and reliable analytical methods, particularly in the context of food safety and migration studies.

Determination of particle number concentration by spICP-MS

The technique spICP-MS was applied for targeted detection of ZnO NPs by number in the food simulants (Figure 4). The migration solutions were analysed directly by spICP-MS without any pre-treatment, as filtration would have retained the particles. However, this method introduced the risk of residual cellulose contaminating the ICP-MS sample introduction system. Zinc particles were detected in both food simulants. However, it was challenging to determine whether these particles were embedded in NC fragments, if Zn^{2+} was attached to cellulose fibres—thus explaining the detected peaks—or if they existed as free nanoparticles. In fact, it is possible that all three scenarios were occurring simultaneously. In water simulant, the higher number of nanoparticles was detected for ZnO-SP. This can be explained by the simpler morphology of spherical NPs, which facilitated their detection as a regular particle. However, ZnO-FL released more total/ionic Zn as shown earlier (Figure 3) despite showing a lower particle count. This behaviour may be attributed to the larger and irregular structure of flower-shaped NPs, meaning that each particle contains a greater amount of Zn and, upon dissolution, contributes more significantly to the ionic fraction compared to spherical NPs.

Moreover, particles were detected in the control sample, which was expected to contain no ZnO NPs. This is likely due to residual particles from prior analyses adhering to the sample-introduction system. In samples with significantly higher

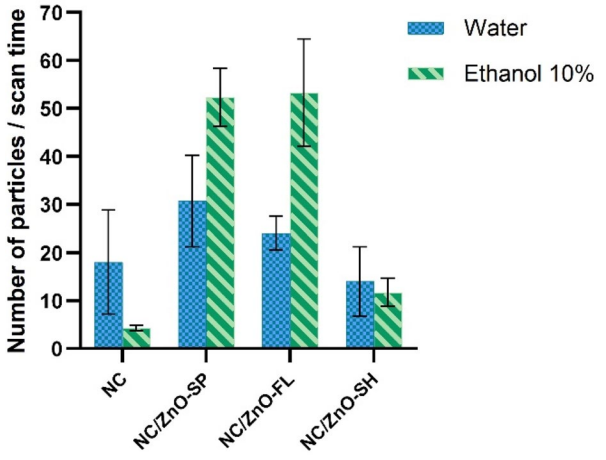

Figure 4. Number of particles per scan time detected by spICP-MS after a contact of 60 °C for 10 days of the NC and NC/ZnO NPs films with water and ethanol 10% food simulants. NC/ZnO-SP - nanocellulose film with spherical ZnO NPs; NC/ZnO-FL - film with flower-like ZnO NPs; NC/ZnO-SH - film with sheet-like ZnO NPs.

particle concentrations (1000–2000 particles per scan), such contamination is negligible. However, in the samples analysed in this study, distinguishing particles originating from the sample-introduction system from those in the actual sample proved challenging. Despite this limitation, a significant increase in spherical and the flower-shaped particles was observed. Furthermore, the higher results for ethanol 10% as compared to water also suggest that cellulose particles may interfere with the zinc particles measurement. Other studies using spICP-MS have reported a significant challenge for detecting and characterising NPs in diverse matrices due to strong spectral interferences (Vidmar 2021). As mentioned earlier, to achieve statistically relevant results, more than 1000 particles would need to be detected per scan time. However, the current data only reveal between 15 and 60 particles, making it impossible to use these values quantitatively.

Investigations of nanoparticles migration from FCMs into food simulants using spICP-MS has been conducted previously (Jokar et al. 2018; Bastardo-Fernández et al. 2024). Studies have applied spICP-MS to detect both ZnO NPs and dissolved Zn in food matrices (Santos et al. 2024). However, it has several limitations, as the dissolved Zn signal overlaps with the nanoparticle signal, directly interfering with the analysis. In these circumstances, only larger particles or agglomerates can be distinguished from dissolved Zn. A study analysed silver release from commercially available plastic food containers into food simulants, performing ICP-MS for total Ag and spICP-MS for nano-silver detection (Mackevica et al. 2016). However, smaller particles might not be accurately detected and quantified. Other studies have applied an ion exchange column to remove dissolved Zn from the samples before analysis by spICP-MS, enabling the quantification and characterisations of ZnO NPs at very low concentrations in natural waters (Hadioui et al. 2015; Fréchette-Viens et al. 2019). This approach seems like a good solution to quantify only the nanoform of the particles. However, its efficiency in food simulants may vary, and its application requires further investigation.

Microscopic visualisation of particles in films and food simulants via transmission electron microscopy

Microscopy observations were performed as a complementary technique to directly visualise ZnO NPs in both films and water food simulant. TEM micrographs confirmed the presence and distribution of ZnO NPs along the migration experiments, thus providing a more comprehensive assessment of their transfer behaviour (Figure 5). The results show that ZnO NPs with different morphologies were successfully incorporated into NC matrix, although some degree of agglomeration among the fibres was observed. After 10 days of contact with water simulant at 60 °C, NPs remained embedded within the NC fibres across all morphologies, suggesting that nanoparticle migration was not complete under the experimental conditions. In parallel, TEM analysis of the entire water food simulant volume (100 mL) after contact revealed the presence of ZnO NPs aggregates as well as numerous cellulose fibres fragments containing embedded NPs. These findings suggest that the signals detected from spICP-MS are associated with both free ZnO NPs (indicating nanoparticles migration) and ZnO NPs embedded in NC filaments (indicating degradation of matrix rather than migration).

The TEM images provide an indicative visualisation of the spatial distribution of the nanoparticles, showing how they may interact with the cellulose fibres and become incorporated into the matrix. It is important to note that ZnO NPs incorporated in a dense NC network may show reduced contrast after film formation. Therefore, distinguishing between the particle and fibres may be less clear. This effect is stronger after contact with water due to partial NP dissolution. Differences in nanoparticle aggregation and dispersion across morphologies suggest that particle shape may also influence migration behaviour. However, it is important to note that while these images confirm the presence of ZnO NPs, they do not provide quantitative data on the extent of nanoparticle migration. Additionally, the micrographs revealed possible structural changes in NC matrix, which appeared more loosened after exposure to the simulant, indicating partial

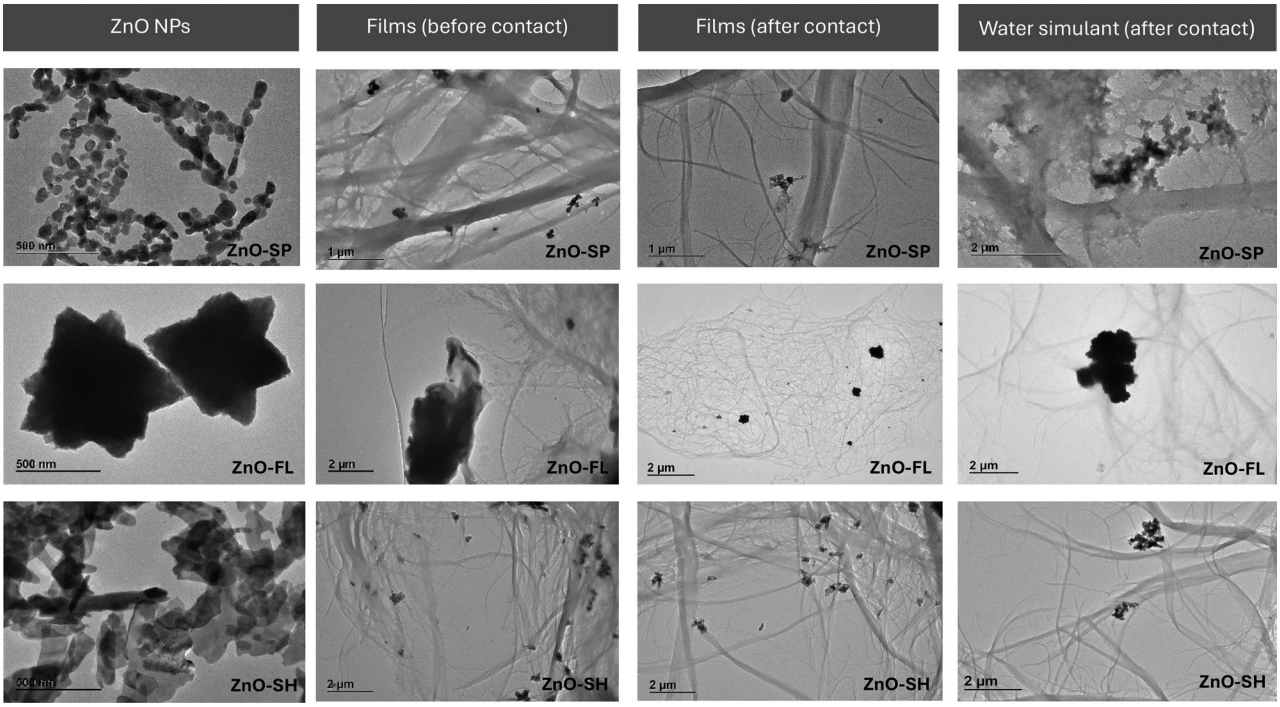

Figure 5. TEM micrographs of ZnO NPs, NC/ZnO NPs films before and after 10 d/ 60 °C contact, and water food simulant after 10 d/ 60 °C contact.

degradation, which may influence the retention or release of ZnO NPs.

The combination of TEM and spICP-MS has been applied in previous studies to confirm the presence of nanoparticles in migration solutions. However, these works were limited to plastic materials and focused on silver (Mackevica et al. 2016) and copper (Mackevica et al. 2016; Zhang et al. 2020), rather than in zinc oxide nanoparticles. Another study examined the migration of ZnO NPs from polybutylene adipate-co-terephthalate (PBAT)/thermoplastic starch (TPS) films using ICP-optical emission spectrometry complemented with SEM analysis (Bumbudsanpharoke et al. 2024). The exposure to a 3% acetic acidic food simulant caused visible surface alterations, associated with pore formation and ZnO dissolution within the film matrix.

Influence of food simulant on total Zn migration

Food simulant properties, such as pH and hydrophilicity, influence Zn migration kinetics, reflecting the material's behaviour in different food matrices scenarios. Overall, the results showed that total Zn migration was consistently higher in water compared to ethanol 10% (Figures 2, 3, and S2). Multiple linear regression analysis of data collected after day 4 demonstrated higher levels of Zn migration, across all shapes, in water food simulant compared to ethanol 10%, with time serving as the controlled variable.

The lower migration in ethanol 10% may be attributed to the lower solubility of Zn species in ethanol compared to water (Soares Silva et al. 2023a). In addition, the greater swelling capacity of cellulose fibres in water likely facilitates higher Zn release (Hubbe et al. 2024). Consistent results are reported in the literature: increasing the ethanol concentration in the food simulant led to a decrease in Zn migration from bacterial nanocellulose films containing ZnO NPs (Soares Silva et al. 2023b).

The migration pattern of NC/ZnO-FL and, to a lesser extent, the NC/ZnO-SP films, exhibited a higher initial migration rate for ethanol 10% within the first 24 h, showing afterwards a decrease in the concentration, suggesting transfer of zinc back to the cellulosic matrix (possible reabsorption). Possibly a burst release effect in the ethanolic medium, likely associated with a faster extraction of loosely bound Zn species or weak interactions

in the film occurs initially. However, after this initial peak, Zn migration in ethanol rapidly decreased and stabilised at lower levels than those observed in water. For the NC/ZnO-SH films, this initial peak was not pronounced, and both simulants resulted in similar early migration levels although with high values for water at later stages. These findings highlight the different patterns of migration of zinc from cellulose matrices, as compared to patterns typically observed in migration kinetics from polymeric matrices (Poças et al. 2008; Bott et al. 2014b).

Similar studies have investigated the migration behaviour of ZnO NPs from PBAT/TPS films but using acetic acid 3% and ethanol 10% as the food simulant (Bumbudsanpharoke et al. 2024). The Zn migration was considerably higher in acetic acid compared to ethanol simulant, as could be expected. In fact, the use of acidic simulant promotes complete dissolution of ZnO NPs from the film, leading to its conversion into the ionic form, which can be comparable to the acidification step of the present study.

Effect of temperature on total Zn migration

The influence of temperature on total Zn migration kinetics from NC/ZnO-SP films was investigated using distilled water as a food simulant at 8, 23 and 60 °C over a period of 35 days (Figure 6). These temperatures were selected to represent refrigerated storage, typical ambient scenario, and a standard accelerated migration conditions, respectively. The results showed that temperature significantly influenced Zn migration behaviour, although the observed trend did not follow the conventional expectation in the scientific community that mass transfer generally increases with temperature.

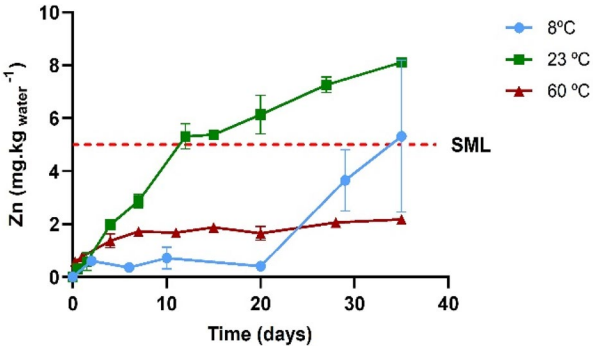

Figure 6. Total Zn migration from NC/ZnO-SP into water food simulant at 8 °C, 23 °C, and 60 °C during 35 days.

At 23 °C, Zn migration exhibited a continuous and progressive increase over time, reaching the highest concentration among the tested conditions (8.72 mg kg^{-1}). A linear regression model estimated the migration rate at 0.253 mg kg^{-1} day^{-1} (R^2 = 0.9; 95%CI, ranging from 0.218 to 0.287). The SML of 5 mg kg^{-1} food was exceeded from day 12 onwards, indicating potential regulatory non-compliance under prolonged room-temperature storage. At 8 °C, migration occurred at a significantly slower rate, with a pronounced increase after the 20th day. This pattern was best described by a cubic model (R^2 = 0.87), suggesting that longer contact times at refrigeration temperatures could eventually result in comparable migration levels, although remaining below the SML within the studied period. Unexpectedly, migration at 60 °C was intermediate and stabilised early in the experiment, displaying a lower initial rate compared to the rate at 23 °C (95% CI for slope ranging 0.020 to 0.055). This contrasts with the well-established behaviour of migration from plastics, where increasing temperature typically enhances mass transfer rates (Franz & Störmer 2008; Hoekstra et al. 2015). Higher temperatures provide more kinetic energy to atoms, enhancing their mobility within the material and thereby promoting Zn release (Pochiraju et al. 2008; Wu 2024). To verify this unexpected trend, the migration experiment was independently repeated under identical conditions, and the results were consistent with the initial findings, confirming the reproducibility of this behaviour. A similar unexpected temperature–migration relationship has also been reported for silver migration from PVC nanocomposites, where higher temperatures were associated with lower migration levels, possibly due to nanoparticle crosslinking with polymer chains (Cushen et al. 2013). In both cases, such counterintuitive behaviour suggests that matrix-specific physicochemical changes at elevated temperatures may hinder nanoparticle release.

The migration from cellulosic materials differs fundamentally from plastics due to their heterogeneous and porous nature, where mass transfer

involves adsorption, desorption, and diffusion through air pores (Poças et al. 2011; Cushen et al. 2013; Hauder et al. 2013). In this work, the observed decrease in Zn migration at higher temperatures (60 °C), suggests that specific factors may be influencing the process, including ZnO solubility, nanoparticle aggregation, and potential modifications of the matrix. At higher temperature, the cellulose material may undergo rearrangement, densification or crosslinking modifications, reducing swelling and porosity, thus hindering Zn mobility. Reduced swelling of cellulose films as temperature increased from 25 °C to 39 °C has been reported (Torstensen et al. 2022). Heating above 150 °C was reported to induce irreversible changes in cellulose nanofibre structures and permeability, affecting their physicochemical properties (Niskanen et al. 2022). Furthermore, dissolution of ZnO NPs releases Zn^{2+}, but several studies have shown that higher temperatures can promote nanoparticle aggregation (Majedi et al. 2013; Yung et al. 2017). Aggregation reduces both particle mobility and the available surface area for dissolution, thereby limiting Zn^{2+} release.

Overall, these findings indicate that while temperature is a key driver of Zn migration, the relationship is not linear for NC/ZnO-SP composites and deviates from the behaviour observed in polymeric systems. The reduced migration at 60 °C suggests that processing or storage under elevated temperatures could, counterintuitively, limit Zn release—although such conditions may also induce material property changes with other implications for packaging performance.

Modelling migration of zinc

Nanoparticle migration from FCM to food simulants and real foods remains underexplored, and the available migration studies that apply mathematical models are limited and often inconclusive regarding the migrating species form (total, ionic, or nanoparticle form). A short literature review was carried out to identify existing studies reporting nanoparticle migration together with modelling strategies in FCM, providing a basis for selecting and applying appropriate models. This search was performed in databases for 2013 to 2025, using general keywords such as 'nanoparticle migration', 'mathematical modelling', 'food packaging', and 'food contact materials'. Relevant studies found are summarised in Table S1.

The identified literature included studies on different polymer matrices, such as low-density polyethylene (LDPE), polystyrene (PS), polylactic acid (PLA), and starch incorporating nanoparticles such as Ag, ZnO, TiO_2, and carbon black. Migration was tested in several food simulants, including ethanolic, acidic, and aqueous media, and a case of a real food (apple juice) was also reported (Jokar et al. 2016). Migration kinetics were most consistently described by mechanistic Fickian second law (Heydari-Majd et al. 2019; Tang et al. 2020; Ortega et al. 2022), with diffusion coefficients estimated *via* Piringer's or Stokes–Einstein equation (Bott et al. 2014c, 2014a, 2014b). Additionally, semi-empirical and empirical models have been applied to better explain the early-stage release behaviour. The Peppas model has been frequently used to describe the initial burst release (Von Goetz et al. 2013; Heydari-Majd et al. 2019; Kim et al. 2019; Ortega et al. 2022), while the Weibull model has provided flexible fits for a wide range of kinetic profiles (Heydari-Majd et al. 2019; Ortega et al. 2022). In some cases, the Elovich model has been employed to account for heterogeneous diffusion coupled with adsorption processes (Hannon et al. 2017; Kim et al. 2019). Other empirical approaches, such as first and second order models, have also been used to describe different migration mechanisms including adsorption/desorption processes and site saturation (Jokar et al. 2016; Hannon et al. 2017). Temperature is known to strongly influence migration rates, and some studies have applied Arrhenius and van't Hoff analyses to describe this effect, respectively in the diffusion and partition coefficients (Hannon et al. 2017; Heydari-Majd et al. 2019; Kim et al. 2019). Studies applying semi-empirical/empirical models rather than Fickian diffusion used both Arrhenius and van't Hoff analyses, to describe the effect of temperature in different model parameters (release rate constants, second-order rate constants, or equilibrium constants).

Overall, the migration mechanism can vary substantially depending on different factors such

as the NPs incorporated, the nature of polymer matrix, and the type of food simulant or real food tested. Consequently, migration is not necessarily governed by purely Fickian diffusion, but may also involve other processes such as desorption, dissolution, or matrix degradation (Duncan and Pillai 2015). This variability in mechanisms represents a key scientific challenge, as it makes difficult the selection of appropriate models.

Most of the NPs incorporated in the packaging materials reported in the literature are silver-based, with only one study focusing on ZnO (Heydari-Majd et al. 2019). Modelling has been performed mainly using the total or ionic concentrations of the metal. Although a low number of studies have directly quantified migration of the nanoparticle form (using spICP-MS and Asymmetric Flow Field-Flow Fractionation (AF4) with Multi-Angle Light Scattering (MALS) AF4-MALS), none has applied a mathematical model to predict its kinetic profile (Von Goetz et al. 2013; Bott et al. 2014c).

Building on these insights, migration data of this study were fitted to a mechanistic Fickian model and to the empirical Weibull equation. As direct quantification of the nanoparticle form was not feasible, modelling was performed on total zinc concentrations (including both dissolved and particulate fractions) in water food simulant at 60 °C. The results are presented in Table 2 and Figure 7 which compare the performance of both models and the migration behaviour of different ZnO NPs morphologies. For ZnO-FL films, the migration profile could not be satisfactorily described by either model, and therefore the corresponding fitting curves are not shown in Figure 7.

For ZnO-SP, both models fitted well, showing identical goodness-of-fit parameters (MSE = 0.025; R^2 = 0.94 for both), with the slowest approach to equilibrium ($\tau = 2.01$). ZnO-FL exhibited the highest effective diffusivity ($D = 1.21 \times 10^{-15}$ $m^2 s^{-1}$), but the fits were very poor (R^2 = 0.63 for both; MSE ≈ 0.16–0.17), showing less accurate prediction and lower variance explained by the models. This irregular migration behaviour may be attributed to the initial peak of Zn release followed by partial reabsorption. In addition, heterogeneities in particle distribution, agglomeration phenomena, or irregularities at the film/simulant interface could also lead to deviations from ideal Fickian or Weibull behaviour. For ZnO-SH, the Fick model provided a better fit than the Weibull model, with MSE = 0.025 and R^2 = 0.83, compared to MSE = 0.076 and R^2 = 0.07, respectively. This shape displayed a burst effect with the fastest migration rate (1.82×10^{-5} mg $kg^{-1} day^{-1}$), which is consistent with the β values obtained from the Weibull model (ZnO-SH showed the highest β (0.68)), indicating a faster onset of release. In fact, this may explain the

Table 2. Parameters of Fick and Weibull models describing total Zn migration from NC/ZnO films into water simulant at 60 °C.

Model	Parameter	ZnO-SP	ZnO-FL	ZnO-SH
Fick	M∞ (mg kg^{-1})	1.73	1.62	1.10
	D ($m^2 s^{-1}$)	1.48×10^{-16}	1.21×10^{-15}	3.0×10^{-16}
	MSE	0.025	0.161	0.025
	R^2	0.94	0.63	0.83
Weibull	M∞ (mg kg^{-1})	1.82	1.54	1.13
	τ (days)	2.01	0.02	0.62
	β	0.59	0.39	0.68
	MSE	0.025	0.168	0.076
	R^2	0.94	0.63	0.70
Initial migration rate* (mg kg^{-1} day^{-1})		7.50×10^{-6}	8.13×10^{-6}	1.82×10^{-5}

*Calculated from the slope of the first three experimental points (up to 1 day).

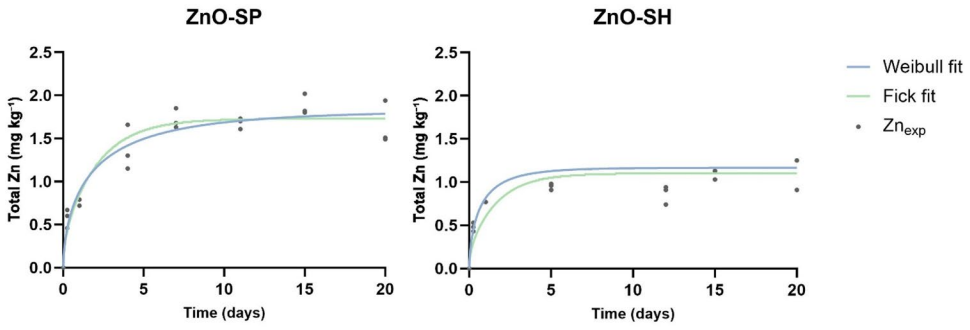

Figure 7. Profile migration of total Zn from NC/ZnO-SP and NC/ZnO-SH into water food simulant over 20 days at 60 °C. Experimental data are compared with fitting Fick's diffusion and the Weibull models.

superior antimicrobial activity previously reported, by rapidly releasing Zn^{2+} ions and ROS species (Mendes et al. 2024, 2025). Achieving inhibitory levels early in the microbial growth lag phase can suppress cell proliferation before colonisation becomes established.

Differences in the release behaviour among ZnO NPs morphologies highlight the influence of nanoparticles type and surface chemistry on migration kinetics, providing guidance for future packaging optimisation. The migration of Zn corresponded to about 1%–2% of the initially incorporated amount for the SP and SH films, while for the FL film it reached approximately 3.5%. The more controlled and sustained release was observed for ZnO-SP particles, with a stable kinetic profile, consistent with their uniform, spherical morphology. A similar study incorporated ZnO NPs into a PLA matrix and quantified Zn release by AAS, analysing the data with Fick's diffusion model, the Korsmeyer–Peppas power law, and a Weibull fit (Heydari-Majd et al. 2019). Compared with PLA, the cellulose films in water at 60 °C show diffusion coefficients within the mid–upper range reported for PLA (lower than PLA/95% EtOH at 40 °C but higher than PLA/10–20% EtOH). Both datasets yield Weibull β parameters < 1 consistent with the high initial rate of release. Nevertheless, comparison between the two studies is limited by the different conditions employed, including polymer type, simulant polarity, and temperature and is only indicative.

Conclusions

This study provides a comprehensive evaluation of Zn migration from NC/ZnO films, addressing critical knowledge gaps in cellulose-based food packaging systems. The combination of analytical techniques (AAS, ICP-MS, spICP-MS, and TEM) enabled a comprehensive analysis of both ionic and nanoparticulate zinc.

Migration occurred predominantly as ionic Zn^{2+}, with all values remaining below the SML of 5 mg kg^{-1} of food established by European legislation. Acidification and filtration approaches using AAS and ICP-MS, respectively, indicated minimal nanoparticle transfer. Although the porous structure of NC facilitated Zn^{2+} diffusion, it also contributed to the partial retention of nanoparticles. The migration behaviour was influenced by nanoparticle morphology, simulant polarity, and temperature. Flower-shaped ZnO NPs exhibited the highest total Zn release in water food simulant (3.07 mg kg^{-1}), whereas spherical particles showed the most stable and sustained profile. Water simulant promoted higher migration than ethanol 10%, highlighting the influence of simulant polarity and swelling. Unexpectedly, Zn release was lower at 60 °C than at 23 °C for ZnO-SP in water food simulant, suggesting that thermally induced densification of the cellulose matrix may limit zinc diffusion. The highest Zn migration was observed at 23 °C, with values exceeding the SML after 12 days of storage, indicating that prolonged room temperature storage could raise potential safety concerns.

This work addressed a critical knowledge gap by applying kinetic modelling to describe Zn migration from nanocellulose-based nanocomposite films, a field where only a limited number of studies exist and most of them are restricted to conventional plastics. By combining a short literature review with new experimental data, this study contributes to advancing the understanding of nanoparticle migration in bio-based systems. Modelling confirmed that Zn migration was predominantly diffusion-driven, with Fickian fits yielding diffusion coefficients in the 10^{-16}–10^{-15} m^2 s^{-1} range and Weibull β parameter < 1, consistent with burst-type release followed by slower diffusion. However, clear morphology-dependent behaviours were observed: spherical ZnO showed the most stable release profile with good agreement across both models, while flower-shaped particles exhibited the highest diffusivity but poor model fits, likely due to reabsorption or heterogeneous particle distribution. These results demonstrate that migration is not always governed by purely Fickian diffusion, as processes such as desorption, dissolution, reabsorption, or matrix degradation may contribute, particularly in porous bio-based systems. This variability represents a key scientific challenge, as it complicates the choice of appropriate models and underscores the need for further investigations.

Overall, NC/ZnO films demonstrated controlled Zn^{2+} migration aligned with active packaging functionalities, but the presence of ZnO NPs in food simulants could not be fully excluded. Given the absence of EFSA-specific guidance for nanoparticle migration in bio-based materials, further research is required to clarify release mechanisms, standardise analytical protocols, and conduct full risk assessments. These findings support the potential of NC/ZnO nanocomposites as sustainable food packaging, while underscoring the importance of balancing antimicrobial efficacy with safety and regulatory compliance. Future research should focus on real food matrices, long-term storage scenarios effects, and the development of advanced analytical methods to improve migration models and support regulatory framework.

Acknowledgments

Experimental data were in part generated under the Framework for Access to the Joint Research Centre Physical Research Infrastructures of the European Commission (Project: PackINZnO–Effect of different morphologies of zinc oxide nanoparticles in migration from nanocellulose nanocomposite), Research Infrastructure Access Agreement N◦ 36689/6; Call 2022-1-RD-Nanobiotech Declaration of competing interest.

Authors' contributions

Credit: **Ana Rita Mendes**: Formal analysis, Investigation, Methodology, Writing – original draft; **Otmar Geiss**: Investigation, Methodology, Writing – review & editing; **Ivana Bianchi**: Investigation, Methodology, Writing – review & editing; **Jessica Ponti**: Investigation, Methodology, Writing – review & editing; **Ana Matos**: Formal analysis, Writing – review & editing; **Cristina L. M. Silva**: Writing – review & editing; **Fátima Poças**: Conceptualization, Resources, Supervision, Writing – review & editing.

Disclosure statement

The authors declare no conflicts of interest.

Funding

This work was supported by National Funds from FCT - Fundação para a Ciência e a Tecnologia through projects UID/50016/2025 and LA/P/0076/2020 (https://doi.org/10.54499/LA/P/0076/2020), and the grant UI/BD/151387/2021 (Ana Rita Mendes).

Data availability statement

Data will be made available on request.

References

Anvar AA, Ahari H, Ataee M. 2021. Antimicrobial properties of food nanopackaging: a new focus on foodborne pathogens. Front Microbiol. 12:690706. https://doi.org/10.3389/fmicb.2021.690706

Bastardo-Fernández I et al. 2024. Assessment of TiO_2 (nano) particles migration from food packaging materials to food simulants by single particle ICP-MS/MS using a high efficiency sample introduction system. NanoImpact. 34:100503. https://doi.org/10.1016/j.impact.2024.100503

Bayer IS. 2023. Controlled drug release from nanoengineered polysaccharides. Pharmaceutics. 15(5):1364. https://doi.org/10.3390/pharmaceutics15051364

Bott J, Störmer A, Franz R. 2014a. A comprehensive study into the migration potential of nano silver particles from food contact polyolefins. In: Duncan TV, editor. Silver nanoparticles in food: safety and applications. Washington, DC: American Chemical Society; p. 51–70.

Bott J, Störmer A, Franz R. 2014b. A model study into the migration potential of nanoparticles from plastics nanocomposites for food contact. Food Packag Shelf Life. 2(2):73–80. https://doi.org/10.1016/j.fpsl.2014.08.001

Bott J, Störmer A, Franz R. 2014c. Migration of nanoparticles from plastic packaging materials containing carbon black into foodstuffs. Food Addit Contam Part A Chem Anal Control Expo Risk Assess. 31(10):1769–1782. https://doi.org/10.1080/19440049.2014.952786

Brandsch J, Mercea P, Rüter M, Tosa V, Piringer O. 2002. Migration modelling as a tool for quality assurance of food packaging. Food Addit Contam. 19(sup1):29–41. https://doi.org/10.1080/02652030110058197

Bumbudsanpharoke N et al. 2024. Effect of migration on the functionality of zinc oxide nanoparticle in polybutylene adipate terephthalate/thermoplastic starch films: a food simulant study. Int J Biol Macromol. 263(Pt 1): 130232. https://doi.org/10.1016/j.ijbiomac.2024.130232

Cai H et al. 2017. Migration kinetics of four photo-initiators from paper food packaging to solid food simulants. Food Addit Contam Part A Chem Anal Control Expo Risk Assess. 34(9):1632–1642. https://doi.org/10.1080/19440049.2017.1331470

Cardoso D, Narcy A, Durosoy S, Bordes C, Chevalier Y. 2021. Dissolution kinetics of zinc oxide and its relationship with physicochemical characteristics. Powder Technol. 378:746–759. https://doi.org/10.1016/j.powtec.2020.10.049

Choleva TG, Tsogas GZ, Giokas DL. 2019. Determination of silver nanoparticles by atomic absorption spectrometry after dispersive suspended microextraction followed by oxidative dissolution back-extraction. Talanta. 196:255–261. https://doi.org/10.1016/j.talanta.2018.12.053

Corps Ricardo AI, Avendaño García S, Guzmán Bernardo FJ, Ríos Á, Rodríguez Martín-Doimeadios RC. 2021.

Rapid assessment of silver nanoparticle migration from food containers into food simulants using a qualitative method. Food Chem. 361:130091. https://doi.org/10.1016/j.foodchem.2021.130091

Crank J. 1986. The mathematics of diffusion. 2nd ed. Oxford: Clarendon Press.

Cushen M, Kerry J, Morris M, Cruz-Romero M, Cummins E. 2013. Migration and exposure assessment of silver from a PVC nanocomposite. Food Chem. 139(1–4):389–397. https://doi.org/10.1016/j.foodchem.2013.01.045

Duncan TV, Pillai K. 2015. Release of engineered nanomaterials from polymer nanocomposites: diffusion, dissolution, and desorption. ACS Appl Mater Interfaces. 7(1):2–19. https://doi.org/10.1021/am5062745

EFSA CEF Panel (EFSA Panel on Food Contact Materials, Enzymes, Flavourings and Processing Aids). 2016. Scientific opinion on the safety assessment of the substance zinc oxide, nanoparticles, for use in food contact materials. EFSA J. 14:4408. https://doi.org/10.2903/j.efsa.2016.4408

EFSA CEF Panel (EFSA Panel on Food Contact Materials, Enzymes, Flavourings and Processing Aids). 2015. Scientific opinion on the safety evaluation of the substance zinc oxide, nanoparticles, uncoated and coated with [3-(methacryloxy)propyl]trimethoxysilane, for use in food contact materials. EFSA J. 13:4063. https://doi.org/10.2903/j.efsa.2015.4063

European Commission. 2016. Commission Regulation (EU) 2016/1416 of 24 August 2016 amending and correcting Regulation (EU) No 10/2011 on plastic materials and articles intended to come into contact with food. Off J Eur Union. L230:22–42. https://eur-lex.europa.eu/legal-content/EN/TXT/HTML/?uri=CELEX:32016R1416

Farooq A et al. 2020. Cellulose from sources to nanocellulose and an overview of synthesis and properties of nanocellulose/zinc oxide nanocomposite materials. Int J Biol Macromol. 154:1050–1073. https://doi.org/10.1016/j.ijbiomac.2020.03.163

Franz R, Störmer A. 2008. Migration of plastic constituents. In: Piringer OG, Baner AL, editors. Plastic packaging: interactions with food and pharmaceuticals. 2nd ed. Hoboken: Wiley. p :349–415. https://doi.org/10.1002/9783527621422.ch11

Fréchette-Viens L, Hadioui M, Wilkinson KJ. 2019. Quantification of ZnO nanoparticles and other Zn-containing colloids in natural waters using a high-sensitivity single particle ICP-MS. Talanta. 200:156–162. https://doi.org/10.1016/j.talanta.2019.03.041

Gao Q et al. 2025. Application of nano-ZnO in the food preservation industry: antibacterial mechanisms, influencing factors, intelligent packaging, preservation film and safety. Crit Rev Food Sci Nutr. 65(22):4327–4353. https://doi.org/10.1080/10408398.2024.2387327

Garrido-Romero M, Aguado R, Moral A, Brindley C, Ballesteros M. 2022. From traditional paper to nanocomposite films: analysis of global research into cellulose for food packaging. Food Packag Shelf Life. 31:100788. https://doi.org/10.1016/j.fpsl.2021.100788

Geiss O et al. 2022. Determination of the transport efficiency in spICP-MS analysis using conventional sample introduction systems: an interlaboratory comparison study. Nanomaterials (Basel). 12(4):725. https://doi.org/10.3390/nano12040725

Habib B et al. 2024. Nanoparticles unveiled: a comprehensive review of classification, properties, synthesis, and applications. Int J Adv Res. 12:861–875. https://doi.org/10.21474/IJAR01/19322

Hadioui M, Merdzan V, Wilkinson KJ. 2015. Detection and characterization of ZnO nanoparticles in surface and waste waters using single particle ICP-MS. Environ Sci Technol. 49(10):6141–6148. https://doi.org/10.1021/acs.est.5b00681

Hannon JC et al. 2017. Kinetic desorption models for the release of nanosilver from an experimental nanosilver coating on polystyrene food packaging. Innov Food Sci Emerg Technol. 44:149–158. https://doi.org/10.1016/j.ifset.2017.07.001

Hauder J, Benz H, Rüter M, Piringer O-G. 2013. The specific diffusion behaviour in paper and migration modelling from recycled board into dry foodstuffs. Food Addit Contam Part A Chem Anal Control Expo Risk Assess. 30(3):599–611. https://doi.org/10.1080/19440049.2012.762605

Herrera-Rivera MR et al. 2024. Nanotechnology in food packaging materials: role and application of nanoparticles. RSC Adv. 14(30):21832–21858. https://doi.org/10.1039/D4RA03711A

Heydari-Majd M et al. 2019. Kinetic release study of zinc from polylactic acid based nanocomposite into food simulants. Polym Test. 76:254–260. https://doi.org/10.1016/j.polymertesting.2019.03.040

Hoekstra EJ et al. 2015. Practical guidelines on the application of migration modelling for the estimation of specific migration. Publ Off Eur. Union, Luxembourg, EUR 27529 EN. https://doi.org/10.2788/04517

Huang H, Tang K, Luo Z, Zhang H, Qin Y. 2017. Migration of Ti and Zn from nanoparticle-modified LDPE films into food simulants. FSTR. 23(6):827–834. https://doi.org/10.3136/fstr.23.827

Hubbe MA et al. 2024. Swelling of cellulosic fibers in aqueous systems: a review of chemical and mechanistic factors. BioRes. 19(3):19. https://doi.org/10.15376/biores.19.3.Hubbe

Jokar M, Correia M, Loeschner K. 2018. Behavior of silver nanoparticles and ions in food simulants and low-fat cow milk under migration conditions. Food Control. 89:77–85. https://doi.org/10.1016/j.foodcont.2018.01.023

Jokar M, Loeschner K, Nafchi AM, Research Group for Nano-Bio Science, Division of Food Technology, National Food Institute, Technical University of Denmark (DTU), Søborg, Denmark. 2016. Modeling of silver migration from polyethylene nanocomposite packaging into a food model system using response surface methodology. IJFE. 2:96–102. https://doi.org/10.18178/ijfe.2.2.96-102

Karuppan Perumal MK, Rajasekaran MBS, Rajan Renuka R, Samrot AV, Nagarajan M. 2025. Zinc oxide nanoparticles and their nanocomposites as an imperative coating for smart food packaging. Appl Food Res. 5(1):100849. https://doi.org/10.1016/j.afres.2025.100849

Kim I et al. 2022. ZnO nanostructures in active antibacterial food packaging: preparation methods, antimicrobial mechanisms, safety issues, future prospects, and challenges. Food Rev Int. 38(4):537–565. https://doi.org/10.1080/87559129.2020.1737709

Kim MH et al. 2019. Kinetic and thermodynamic studies of silver migration from nanocomposites. J Food Eng. 243:1–8. https://doi.org/10.1016/j.jfoodeng.2018.08.028

Kumar R, Umar A, Kumar G, Nalwa HS. 2017. Antimicrobial properties of ZnO nanomaterials: a review. Ceram Int. 43(5):3940–3961. https://doi.org/10.1016/j.ceramint.2016.12.062

Kwabena DE, Wee BS, Chin SF, Kok KY, Maligan MF. 2021. Zinc oxide nanoparticles synthesis methods and its effect on morphology: a review. Biointerface Res Appl Chem. 12:4261–4292. https://doi.org/10.33263/BRIAC123.42614292

Lebaka VR, Ravi P, Reddy MC, Thummala C, Mandal TK. 2025. Zinc oxide nanoparticles in modern science and technology: multifunctional roles in healthcare, environmental remediation, and industry. Nanomaterials (Basel). 15(10):754. https://doi.org/10.3390/nano15100754

Mackevica A, Olsson ME, Hansen SF. 2016. Silver nanoparticle release from commercially available plastic food containers into food simulants. J Nanopart Res. 18(1):5. https://doi.org/10.1007/s11051-015-3313-x

Majedi SM, Lee HK, Kelly BC. 2013. Role of water temperature in the fate and transport of zinc oxide nanoparticles in aquatic environment. J Phys Conf Ser. 429:012039. https://doi.org/10.1088/1742-6596/429/1/012039

Mendes AR et al. 2024. Optimizing antimicrobial efficacy: investigating the impact of zinc oxide nanoparticle shape and size. Nanomaterials (Basel). 14(7):638. https://doi.org/10.3390/nano14070638

Mendes AR et al. 2025. Functional properties and safety considerations of zinc oxide nanoparticles under varying conditions. Nanomaterials (Basel). 15(12):892. https://doi.org/10.3390/nano15120892

More S, EFSA Scientific Committee. et al. 2021a. Guidance on risk assessment of nanomaterials to be applied in the food and feed chain: human and animal health. EFSA J. 19(8):e06768. https://doi.org/10.2903/j.efsa.2021.6768

More S, EFSA Scientific Committee. et al. 2021b. Guidance on technical requirements for regulated food and feed product applications to establish the presence of small particles including nanoparticles. EFSA J. 19(8):e06769. https://doi.org/10.2903/j.efsa.2021.6769

Niskanen I et al. 2022. Optical properties of cellulose nanofibre films at high temperatures. J Polym Res. 29(5):187. https://doi.org/10.1007/s10965-022-03019-0

Noonan GO, Whelton AJ, Carlander D, Duncan TV. 2014. Measurement methods to evaluate engineered nanomaterial release from food contact materials. Compr Rev Food Sci Food Saf. 13(4):679–692. https://doi.org/10.1111/1541-4337.12079

Ortega F, Sobral P, Jios JL, Arce VB, García MA. 2022. Starch nanocomposite films: migration studies of nanoparticles to food simulants and bio-disintegration in soil. Polymers (Basel). 14(9):1636. https://doi.org/10.3390/polym14091636

Österberg M, Henn KA, Farooq M, Valle-Delgado JJ. 2023. Biobased nanomaterials—the role of interfacial interactions for advanced materials. Chem Rev. 123(5):2200–2241. https://doi.org/10.1021/acs.chemrev.2c00492

Pace HE et al. 2011. Determining transport efficiency for the purpose of counting and sizing nanoparticles via single particle inductively coupled plasma mass spectrometry. Anal Chem. 83(24):9361–9369. https://doi.org/10.1021/ac201952t

Panea B, Ripoll G, González J, Fernández-Cuello Á, Albertí P. 2014. Effect of nanocomposite packaging containing different proportions of ZnO and Ag on chicken breast meat quality. J Food Eng. 123:104–112. https://doi.org/10.1016/j.jfoodeng.2013.09.029

Parab AR, Ramlal A, Gopinath SCB, Subramaniam S. 2025. Forging the future of nanotechnology: embracing greener practices for a resilient today and a sustainable tomorrow. Front Nanotechnol. 6:1506665. https://doi.org/10.3389/fnano.2024.1506665

Paul HR, Bera MK, Macke N, Rowan SJ, Tirrell MV. 2024. Quantitative determination of metal ion adsorption on cellulose nanocrystals surfaces. ACS Nano. 18(3):1921–1930. https://doi.org/10.1021/acsnano.3c06140

Piringer OG, Baner AL. 2008. Plastic packaging: interactions with food and pharmaceuticals. 2nd ed. Hoboken: Wiley. https://doi.org/10.1002/9783527621422

Poças F, Franz R. 2018. Overview on European regulatory issues, legislation, and EFSA evaluations of nanomaterials. In: Nanomaterials for food packaging. Amsterdam: Elsevier; p. 277–300.

Poças F. 2018. Migration from packaging and food contact materials into foods. In: Reference module in food science. Amsterdam: Elsevier. https://doi.org/10.1016/b978-0-08-100596-5.21460-1

Poças MF, Oliveira JC, Brandsch R, Hogg T. 2012. Analysis of mathematical models to describe the migration of additives from packaging plastics to foods. J Food Process Engng. 35(4):657–676. https://doi.org/10.1111/j.1745-4530.2010.00612.x

Poças MF, Oliveira JC, Oliveira FAR, Hogg T. 2008. A critical survey of predictive mathematical models for migration from packaging. Crit Rev Food Sci Nutr. 48(10):913–928. https://doi.org/10.1080/10408390701761944

Poças MF, Oliveira JC, Pereira JR, Brandsch R, Hogg T. 2011. Modelling migration from paper into a food simulant. Food Control. 22(2):303–312. https://doi.org/10.1016/j.foodcont.2010.07.028

Pochiraju KV, Tandon GP, Schoeppner GA. 2008. Evolution of stress and deformations in high-temperature polymer

matrix composites during thermo-oxidative aging. Mech Time-Depend Mater. 12(1):45–68. https://doi.org/10.1007/s11043-007-9042-5

Santos LMG et al. 2024. Development of the methodology for the detection and quantification of zinc oxide nanoparticles and dissolved zinc by single-particle inductively coupled plasma mass spectrometry. J Nanopart Res. 26:233. https://doi.org/10.1007/s11051-024-06151-8

Santos RF et al. 2021. Nanofibrillated cellulose and its applications in cement-based composites: a review. Constr Build Mater. 288:123122. https://doi.org/10.1016/j.conbuildmat.2021.123122

Schmidt B et al. 2011. Quantitative characterization of gold nanoparticles by field-flow fractionation coupled online with light scattering detection and inductively coupled plasma mass spectrometry. Anal Chem. 83(7):2461–2468. https://doi.org/10.1021/ac102545e

Seref N, Cufaoglu G. 2025. Food packaging and chemical migration: a food safety perspective. J Food Sci. 90(5):e70265. https://doi.org/10.1111/1750-3841.70265

Sharaby MR, Soliman EA, Abdel-Rahman AB, Osman A, Khalil R. 2022. Novel pectin-based nanocomposite film for active food packaging applications. Sci Rep. 12(1):20673. https://doi.org/10.1038/s41598-022-25192-4

Silva FAGS, Dourado F, Gama M, Poças F. 2020. Nanocellulose bio-based composites for food packaging. Nanomaterials (Basel). 10(10):2041. https://doi.org/10.3390/nano10102041

Singh S et al. 2024. Safety profile of ZnO active packaging PBAT-based biomaterial for food packaging: first tier evaluation. Food Control. 161:110389. https://doi.org/10.1016/j.foodcont.2024.110389

Singh S et al. 2025. Development of bio-based coatings incorporating microfibrillated cellulose, lignin and ionomer dispersions for food contact applications. Packag Technol Sci. 38(8):613–626. https://doi.org/10.1002/pts.2906

Soares Silva FAG et al. 2023. Antimicrobial activity of in-situ bacterial nanocellulose-zinc oxide composites for food packaging. Food Packag Shelf Life. 40:101201. https://doi.org/10.1016/j.fpsl.2023.101201

Soares Silva FAG et al. 2023. Performance of bacterial nanocellulose packaging film functionalised in situ with zinc oxide: migration onto chicken skin and antimicrobial activity. Food Packag Shelf Life. 39:101140. https://doi.org/10.1016/j.fpsl.2023.101140

Souza VGL, Fernando AL. 2016. Nanoparticles in food packaging: biodegradability and potential migration to food: a review. Food Packag Shelf Life. 8:63–70. https://doi.org/10.1016/j.fpsl.2016.04.001

Störmer A, Bott J, Kemmer D, Franz R. 2017. Critical review of the migration potential of nanoparticles in food contact plastics. Trend Food Sci Technol. 63:39–50. https://doi.org/10.1016/j.tifs.2017.01.011

Sun J et al. 2024. Recent advances in cellulose nanofiber modification and characterization and cellulose nanofiber-based films for eco-friendly active food packaging. Foods. 13(24):3999. https://doi.org/10.3390/foods13243999

Tabassum Z, Mohan A, Girdhar M. 2023. Eco-friendly sustainable nanocomposite food packaging materials: recent advancements, challenges, and way forward, In: Modern nanotechnology. Switzerland, Cham: Springer Nature; p. 405–428.

Tang Z, Fan F, Fan C, Jiang K, Qin Y. 2020. The performance changes and migration behavior of PLA/nano-TiO2 composite film by high-pressure treatment in ethanol solution. Polymers (Basel). 12(2):471. https://doi.org/10.3390/polym12020471

Torstensen J et al. 2022. The influence of temperature on cellulose swelling at constant water density. Sci Rep. 12(1):20736. https://doi.org/10.1038/s41598-022-22092-5

Vidmar J. 2021. Detection and characterization of metal-based nanoparticles in environmental, biological and food samples by single particle inductively coupled plasma mass spectrometry. Compr Anal Chem. 93:345–380. https://doi.org/10.1016/bs.coac.2021.02.008

Von Goetz N et al. 2013. Migration of silver from commercial plastic food containers and implications for consumer exposure assessment. Food Addit Contam Part A Chem Anal Control Expo Risk Assess. 30(3):612–620. https://doi.org/10.1080/19440049.2012.762693

Wang J et al. 2025. A review on migration behavior and safety regulation of inorganic nanoparticles in food packaging: multi-scale mechanisms, risk assessment, and innovative strategies. Food Control. 178:111490. https://doi.org/10.1016/j.foodcont.2025.111490

Wu X. 2024. Using Brownian model to study the effect of temperature on diffusion coefficient. TNS. 36(1):48–57. https://doi.org/10.54254/2753-8818/36/20240511

Yang Y et al. 2021. Quantitative detection of zinc oxide nanoparticle in environmental water by cloud point extraction combined ICP-MS. Adsorp Sci Technol. 2021:9958422. https://doi.org/10.1155/2021/9958422

Yung MMN, Kwok KWH, Djurišić AB, Giesy JP, Leung KMY. 2017. Influences of temperature and salinity on physicochemical properties and toxicity of zinc oxide nanoparticles to the marine diatom Thalassiosira pseudonana. Sci Rep. 7(1):3662. https://doi.org/10.1038/s41598-017-03889-1

Zhang L et al. 2025. Multi-functional edible coatings tailored with nanocellulose for perishable fruits. Carbohydr Polym. 358:123520. https://doi.org/10.1016/j.carbpol.2025.123520

Zhang Q et al. 2025. Migration of chemical substances from packaging materials to food. Food Chem. 485:144544. https://doi.org/10.1016/j.foodchem.2025.144544

Zhang Z et al. 2020. Investigating ion-release from nanocomposites in food simulant solutions: case studies contrasting kaolin, CaCO3 and Cu-phthalocyanine. Food Packag Shelf Life. 26:100560. https://doi.org/10.1016/j.fpsl.2020.100560

Zülch A, Piringer O. 2010. Measurement and modelling of migration from paper and board into foodstuffs and dry food simulants. Food Addit Contam Part A Chem Anal Control Expo Risk Assess. 27(9):1306–1324. https://doi.org/10.1080/19440049.2010.483693